An analytical solution for buckling and vibration analysis of functionally graded sandwich beams using a quasi-3D shear deformation theory

Trung-Kien Nguyen[a,*], Thuc P. Vo[b,**], Ba-Duy Nguyen[a,c], Jaehong Lee[d]

[a] *Faculty of Civil Engineering and Applied Mechanics, Ho Chi Minh City University of Technology and Education, 1 Vo Van Ngan Street, Thu Duc District, Ho Chi Minh City, Vietnam*
[b] *Faculty of Engineering and Environment, Northumbria University, Newcastle upon Tyne, NE1 8ST, UK*
[c] *Faculty of Civil Engineering, Thu Dau Mot University, 06 Tran Van On Street, Phu Hoa District, Thu Dau Mot City, Binh Duong Province, Vietnam*
[d] *Department of Architectural Engineering, Sejong University 98 Kunja Dong, Kwangjin Ku, Seoul 143-747, Korea.*

Abstract

This paper presents a Ritz-type analytical solution for buckling and free vibration analysis of functionally graded (FG) sandwich beams with various boundary conditions using a quasi-3D beam theory. It accounts a hyperbolic distribution of both axial and transverse displacements. Equations of motion are derived from Lagrange's equations. Two types of FG sandwich beams namely FG-faces ceramic-core (type A) and FG-core homogeneous-faces (type B) are considered. Numerical results are compared with earlier works and investigated effects of the power-law index, thickness ratio of layers, span-to-depth ratio and boundary conditions on the critical buckling loads and natural frequencies.

Keywords: Functionally graded sandwich beams; A quasi-3D theory; Buckling; Vibration.

1. Introduction

Functionally graded (FG) materials are composite materials formed of two or more constituents whose volume fractions varies continuously in a required direction. The advantages of this material type led to the development of many FG sandwich structures that have no interface problems in comparison with traditional laminated composites. Due to the introduction of material gradients in the faces and core, FG sandwich beams has been employed in aerospace and many other industries. Typically, there are two FG sandwich beams namely homogeneous core-FG faces and FG core-homogeneous faces.

Due to significant shear deformation effect in moderately thick and thick FG beams, three main theories that are the first-order shear deformation beam theory (FSBT), higher-order shear deformation beam theory (HSBT) and quasi-3D shear deformation beam theory are popular used to predict

*Corresponding author, tel.: +848 3897 2092
**Corresponding author, tel.: +44 191 243 7856
Email addresses: kiennt@hcmute.edu.vn (Trung-Kien Nguyen), thuc.vo@northumbria.ac.uk (Thuc P. Vo)

their vibration and buckling responses. The FSBT is the simplest model ([1–6]), however it requires a suitable shear correction factor. To overcome this adverse, the HSBT ([7–19]) refined the distribution of transverse shear stress through the beam depth and consequently no shear correction factor is needed. For thick FG beams, the normal strain effect becomes very important and should be considered ([20]). In order to take into account shear and normal deformations, the quasi-3D theories are developed based on a higher-order variation of both axial and transverse displacements. Based on 1D Carrera's Unified Formulation ([20]), he and his co-workers ([21–23]) investigated various structural problems. As far as the knowledge of the authors, there is still limited work on static, vibration and buckling of FG sandwich beams using a quasi-3D theory. Vo et al. ([24, 25]) developed finite element models to investigate FG sandwich beams using a quasi-3D polynomial theory. Mantari and Yarascab [26–28], and Osofero et al. [29] derived Navier solution for bending, vibration and buckling of FG sandwich beams using non-polynomial quasi-3D theories, respectively.

In this paper, Ritz-type analytical solution for buckling and vibration analysis of FG sandwich beams for various boundary conditions using a quasi-3D shear deformation theory is presented. Lagrangian functional is used to derive equations of motion. Two types of FG sandwich beams namely FG-faces ceramic-core (type A) and FG-core homogeneous-faces (type B) are considered. Numerical results are compared with those reported previously in literature. The effects of the power-law index, span-to-depth ratio and skin-core-skin thickness ratios on the critical buckling loads and natural frequencies of FG sandwich beams are investigated.

2. Theoretical formulation

Consider a FG sandwich beam as shown in Fig. 1, which is made of a mixture of ceramic and metal, with length L and uniform section $b \times h$. Two types of FG sandwich beams namely FG-faces ceramic-core (type A) and FG-core homogeneous-faces (type B) are considered.

2.0.1. Type A: sandwich beams with FG-faces ceramic-core

The faces are made of FG and the core is made of ceramic (Fig. 1a). The volume fraction function of ceramic phase $V_c^{(j)}$ given by:

$$\begin{cases} V_c^{(1)}(z) = \left(\frac{z-h_0}{h_1-h_0}\right)^p & \text{for} \quad z \in [h_0, h_1] \\ V_c^{(2)}(z) = 1 & \text{for} \quad z \in [h_1, h_2] \\ V_c^{(3)}(z) = \left(\frac{z-h_3}{h_2-h_3}\right)^p & \text{for} \quad z \in [h_2, h_3] \end{cases} \quad (1)$$

2.0.2. *Type B: sandwich beams with FG-core homogeneous-faces*

The lower and upper face is made of metal and ceramic, while core layer is made of FG (Fig. 1b). The volume fraction function of ceramic material of the j-th layer $V_c^{(j)}$ defined by:

$$\begin{cases} V_c^{(1)}(z) = 0 & \text{for} \quad z \in [h_0, h_1] \\ V_c^{(2)}(z) = \left(\frac{z-h_1}{h_2-h_1}\right)^p & \text{for} \quad z \in [h_1, h_2] \\ V_c^{(3)}(z) = 1 & \text{for} \quad z \in [h_2, h_3] \end{cases} \tag{2}$$

The material property distribution of FG sandwich beams through the beam depth is given by the power-law form:

$$P(z) = (P_c - P_m)V_c(z) + P_c \tag{3}$$

where P_c and P_m are Young's moduli (E), Poisson's ratio (ν), mass density (ρ) of ceramic and metal materials, respectively.

2.1. *Quasi-3D shear deformation beam theory*

The displacement field of the present theory is given by:

$$u_1(x,z) = u(x) - zw_{,x} + f(z)\theta_x(x) \tag{4a}$$

$$u_3(x,z) = w(x) + g(z)w_z(x) \tag{4b}$$

where the comma indicates partial differentiation with respect to the coordinate subscript that follows; u, w, θ_x and w_z are four variables to be determined; $g(z) = f_{,z}$ where the shape function $f(z)$ is chosen as follows ([18]):

$$f(z) = \cot^{-1}\left(\frac{h}{z}\right) - \frac{16z^3}{15h^3} \tag{5}$$

The nonzero strains associated with the displacement field in Eq. (4) are:

$$\epsilon_{xx}(x,z) = \epsilon_{xx}^0 + z\kappa_{xx}^b + f\kappa_{xx}^s \tag{6a}$$

$$\epsilon_{zz}(x,z) = g_{,z}\epsilon_{zz}^0 \tag{6b}$$

$$\gamma_{xz}(x,z) = g\gamma_{xz}^0 \tag{6c}$$

where ϵ_{xx}^0, κ_{xx}^b, κ_{xx}^s, ϵ_{zz}^0 and γ_{xz}^0 are related with the displacements u, w, θ_x and w_z as follows:

$$\epsilon_{xx}^0(x) = u_{,x}, \quad \kappa_{xx}^b(x) = -w_{,xx}, \quad \kappa_{xx}^s(x) = \theta_{x,x} \tag{7a}$$

$$\epsilon_{zz}^0(x) = w_z \tag{7b}$$

$$\gamma_{xz}^0(x) = \theta_x + w_{z,x} \tag{7c}$$

The strains and stresses are related by the following elastic constitutive equation:

$$\begin{Bmatrix} \sigma_{xx} \\ \sigma_{zz} \\ \sigma_{xz} \end{Bmatrix} = \begin{bmatrix} \bar{Q}_{11} & \bar{Q}_{13} & 0 \\ \bar{Q}_{13} & \bar{Q}_{11} & 0 \\ 0 & 0 & \bar{Q}_{55} \end{bmatrix} \begin{Bmatrix} \epsilon_{xx} \\ \epsilon_{zz} \\ \gamma_{xz} \end{Bmatrix} \tag{8}$$

where

$$\bar{Q}_{11} = \frac{E(z)}{1-\nu^2}, \quad \bar{Q}_{13} = \frac{E(z)\nu}{1-\nu^2}, \quad \bar{Q}_{55} = \frac{E(z)}{2(1+\nu)} \tag{9}$$

2.2. Variational formulation

In order to derive the equations of motion, Lagrangian functional is used:

$$\Pi = \mathcal{U} + \mathcal{V} - \mathcal{K} \tag{10}$$

where $\mathcal{U}$, $\mathcal{V}$ and $\mathcal{K}$ denote the strain energy, work done, and kinetic energy, respectively.

The strain energy of the beam is calculated by:

$$\begin{aligned} \mathcal{U} &= \frac{1}{2}\int_V (\sigma_{xx}\epsilon_{xx} + \sigma_{zz}\epsilon_{zz} + \sigma_{xz}\gamma_{xz})dV \\ &= \frac{1}{2}\int_0^L \Big[Au_{,x}^2 - 2Bu_{,x}w_{,xx} + Dw_{,xx}^2 + 2B^s u_{,x}\theta_{x,x} - 2D^s w_{,xx}\theta_{x,x} + H^s\theta_{x,x}^2 \\ &+ 2(Xu_{,x}w_z - Yw_{,xx}w_z + Y^s\theta_{x,x}w_z) + Zw_z^2 + A_{55}^s(\theta_x^2 + 2\theta_x w_{z,x} + w_{z,x}^2\Big]dx \end{aligned} \tag{11}$$

where

$$(A, B, D, B^s, D^s, H^s, Z) = \sum_{j=1}^{3}\int_{h_{j-1}}^{h_j} \bar{Q}_{11}^{(j)}(z)\left(1, z, z^2, f, fz, f^2, g_{,z}^2\right) bdz \tag{12a}$$

$$(X, Y, Y^s) = \sum_{j=1}^{3}\int_{h_{j-1}}^{h_j} \bar{Q}_{13}^{(j)}(z)\,(1, z, f)\, g_{,z} bdz \tag{12b}$$

$$A_{55}^s = \sum_{j=1}^{3}\int_{h_{j-1}}^{h_j} \bar{Q}_{55}^{(j)}(z) g^2 bdz \tag{12c}$$

The work done by the axial load N_0 can be expressed as:

$$\mathcal{V} = -\frac{1}{2}\int_0^L N_0 w_{,x}^2 dx \tag{13}$$

The kinetic energy is obtained as:

$$
\begin{aligned}
\mathcal{K} &= \frac{1}{2}\int_V \rho(z)(\dot{u}_1^2+\dot{u}_3^2)dV \\
&= \frac{1}{2}\int_0^L \Big[I_0\dot{u}^2 - 2I_1\dot{u}\dot{w}_{,x} + I_2\dot{w}_{,x}^2 + 2J_1\dot{\theta}_x\dot{u} - 2J_2\dot{\theta}_x\dot{w}_{,x} + K_2\dot{\theta}_x^2 + I_0\dot{w}^2 \\
&+ 2L_1\dot{w}\dot{w}_z + L_2\dot{w}_z^2\Big]dx
\end{aligned} \tag{14}
$$

where the differentiation with respect to the time t is denoted by dot-superscript convention; ρ is the mass density of each layer and $(I_0, I_1, I_2, J_1, J_2, K_2, L_1, L_2)$ are the inertia coefficients defined by:

$$
(I_0, I_1, I_2, J_1, J_2, K_2, L_1, L_2) = \sum_{j=1}^{3}\int_{h_{j-1}}^{h_j} \rho^{(j)}\left(1, z, z^2, f, fz, f^2, g, g^2\right) bdz \tag{15}
$$

By substituting Eqs. (11), (13) and (14) into Eq. (10), Lagrangian functional is explicitly expressed as:

$$
\begin{aligned}
\Pi &= \frac{1}{2}\int_0^L \Big[Au_{,x}^2 - 2Bu_{,x}w_{,xx} + Dw_{,xx}^2 + 2B^s u_{,x}\theta_{x,x} - 2D^s w_{,xx}\theta_{x,x} + H^s\theta_{x,x}^2 \\
&+ 2(Xu_{,x}w_z - Yw_{,xx}w_z + Y^s\theta_{x,x}w_z) + Zw_z^2 + A_{55}^s(\theta_x^2 + 2\theta_x w_{z,x} + w_{z,x}^2) - N_0 w_{,x}^2 \\
&- (I_0\dot{u}^2 - 2I_1\dot{u}\dot{w}_{,x} + I_2\dot{w}_{,x}^2 + 2J_1\dot{\theta}_x\dot{u} - 2J_2\dot{\theta}_x\dot{w}_{,x} + K_2\dot{\theta}_x^2 + I_0\dot{w}^2 + 2L_1\dot{w}\dot{w}_z + L_2\dot{w}_z^2)\Big]dx
\end{aligned} \tag{16}
$$

In order to derive the equations of motion, the solution field (u, w, θ_x, w_z) is approximated as the following forms:

$$ u(x,t) = \sum_{j=1}^{m}\psi_j(x)u_j e^{i\omega t} \tag{17a} $$

$$ w(x,t) = \sum_{j=1}^{m}\varphi_j(x)w_j e^{i\omega t} \tag{17b} $$

$$ \theta_x(x,t) = \sum_{j=1}^{m}\psi_j(x)x_j e^{i\omega t} \tag{17c} $$

$$ w_z(x,t) = \sum_{j=1}^{m}\varphi_j(x)y_j e^{i\omega t} \tag{17d} $$

where ω is the frequency of free vibration of the beam, $\sqrt{i} = -1$ the imaginary unit, (u_j, w_j, x_j, y_j) denotes the values to be determined, $\psi_j(x)$ and $\varphi_j(x)$ are the shape functions. To derive analytical solutions, the shape functions $\psi(x)$ and $\varphi(x)$ are chosen for various boundary conditions (S-S: simply supported, C-C: clamped-clamped, and C-F: clamped-free beams) as follows:

$$ \psi(x) = x^{j-1},\ \varphi(x) = x^{j-1} \tag{18} $$

In order to impose the various boundary conditions, the method of Lagrange multipliers can be used so that the Lagrangian functional of the problem is rewritten as follows:

$$\Pi^* = \Pi + \beta_i \hat{u}_i(\bar{x}) \tag{19}$$

where β_i are the Lagrange multipliers which are the support reactions of the problem, $\hat{u}_i(\bar{x})$ denote the values of prescribed displacement at location $\bar{x} = 0, L$. By substituting Eq. (17) into Eq. (16), and using Lagrange's equations:

$$\frac{\partial \Pi^*}{\partial q_j} - \frac{d}{dt}\frac{\partial \Pi^*}{\partial \dot{q}_j} = 0 \tag{20}$$

with q_j representing the values of $(u_j, w_j, x_j, y_j, \beta_j)$, that leads to:

$$\left(\begin{bmatrix} \mathbf{K}^{11} & \mathbf{K}^{12} & \mathbf{K}^{13} & \mathbf{K}^{14} & \mathbf{K}^{15} \\ {}^T\mathbf{K}^{12} & \mathbf{K}^{22} & \mathbf{K}^{23} & \mathbf{K}^{24} & \mathbf{K}^{25} \\ {}^T\mathbf{K}^{13} & {}^T\mathbf{K}^{23} & \mathbf{K}^{33} & \mathbf{K}^{34} & \mathbf{K}^{35} \\ {}^T\mathbf{K}^{14} & {}^T\mathbf{K}^{24} & {}^T\mathbf{K}^{34} & \mathbf{K}^{44} & \mathbf{K}^{45} \\ {}^T\mathbf{K}^{15} & {}^T\mathbf{K}^{25} & {}^T\mathbf{K}^{35} & {}^T\mathbf{K}^{45} & \mathbf{0} \end{bmatrix} - \omega^2 \begin{bmatrix} \mathbf{M}^{11} & \mathbf{M}^{12} & \mathbf{M}^{13} & \mathbf{0} & \mathbf{0} \\ {}^T\mathbf{M}^{12} & \mathbf{M}^{22} & \mathbf{M}^{23} & \mathbf{M}^{24} & \mathbf{0} \\ {}^T\mathbf{M}^{13} & {}^T\mathbf{M}^{23} & \mathbf{M}^{33} & \mathbf{0} & \mathbf{0} \\ \mathbf{0} & {}^T\mathbf{M}^{24} & \mathbf{0} & \mathbf{M}^{44} & \mathbf{0} \\ \mathbf{0} & \mathbf{0} & \mathbf{0} & \mathbf{0} & \mathbf{0} \end{bmatrix} \right) \begin{Bmatrix} \mathbf{u} \\ \mathbf{w} \\ \boldsymbol{\theta}_x \\ \mathbf{w}_z \\ \boldsymbol{\beta} \end{Bmatrix} = \begin{Bmatrix} \mathbf{0} \\ \mathbf{0} \\ \mathbf{0} \\ \mathbf{0} \\ \mathbf{0} \end{Bmatrix} \tag{21}$$

where the components of the stiffness matrix $\mathbf{K}$ and the mass matrix $\mathbf{M}$ are given as follows:

$$\begin{aligned}
K_{ij}^{11} &= A\int_0^L \psi_{i,x}\psi_{j,x}\,dx, K_{ij}^{12} = -B\int_0^L \psi_{i,x}\varphi_{j,xx}\,dx, K_{ij}^{13} = B^s\int_0^L \psi_{i,x}\psi_{j,x}\,dx \\
K_{ij}^{14} &= X\int_0^L \psi_{i,x}\varphi_j\,dx, K_{ij}^{22} = D\int_0^L \varphi_{i,xx}\varphi_{j,xx}\,dx - N^0\int_0^L \varphi_{i,x}\varphi_{j,x}\,dx \\
K_{ij}^{23} &= -D^s\int_0^L \varphi_{i,xx}\psi_{j,x}\,dx, K_{ij}^{24} = -Y\int_0^L \varphi_{i,xx}\varphi_j\,dx \\
K_{ij}^{33} &= H^s\int_0^L \psi_{i,x}\psi_{j,x}\,dx + A_{55}^s\int_0^L \psi_i\psi_j\,dx, K_{ij}^{34} = Y^s\int_0^L \psi_{i,x}\varphi_j\,dx + A_{55}^s\int_0^L \psi_i\varphi_{j,x}\,dx \\
K_{ij}^{44} &= Z\int_0^L \varphi_i\varphi_j\,dx + A_{55}^s\int_0^L \varphi_{i,x}\varphi_{j,,x}\,dx \\
M_{ij}^{11} &= I_0\int_0^L \psi_i\psi_j\,dx, M_{ij}^{12} = -I_1\int_0^L \psi_i\varphi_{j,x}\,dx, M_{ij}^{13} = J_1\int_0^L \psi_i\psi_j\,dx \\
M_{ij}^{22} &= I_0\int_0^L \varphi_i\varphi_j\,dx + I_2\int_0^L \varphi_{i,x}\varphi_{j,x}\,dx, M_{ij}^{23} = -J_2\int_0^L \varphi_{i,x}\psi_j\,dx \\
M_{ij}^{24} &= L_1\int_0^L \varphi_i\varphi_j\,dx, M_{ij}^{33} = K_2\int_0^L \psi_i\psi_j\,dx, M_{ij}^{44} = L_2\int_0^L \psi_i\psi_j\,dx
\end{aligned} \tag{22}$$

and the components of $\mathbf{K}^{15}$, $\mathbf{K}^{25}$, $\mathbf{K}^{35}$ and $\mathbf{K}^{45}$ depend on number of boundary conditions and associated prescribed displacements (Table 1). For C-C beams, these stiffness components are given by:

$$
\begin{aligned}
K_{i1}^{15} &= \psi_i(0),\, K_{i2}^{14} = \psi_i(L),\, K_{ij}^{14} = 0 \quad \text{with}\, j = 3, 4, ..., 10 \\
K_{i3}^{25} &= \varphi_i(0),\, K_{i4}^{25} = \varphi_i(L),\, K_{i5}^{25} = \varphi_{i,x}(0),\, K_{i6}^{25} = \varphi_{i,x}(L), K_{ij}^{25} = 0 \quad \text{with}\, j = 1, 2, 7, ..., 10 \\
K_{i7}^{35} &= \psi_i(0),\, K_{i8}^{35} = \psi_i(L),\, K_{ij}^{35} = 0 \quad \text{with}\, j = 1, 2, ..., 6, 9, 10 \\
K_{i9}^{45} &= \varphi_i(0),\, K_{i10}^{45} = \varphi_i(L),\, K_{ij}^{45} = 0 \quad \text{with}\, j = 1, 2, ..., 8
\end{aligned} \tag{23}
$$

The solution of Eq. (21) will allow to calculate the critical buckling loads and natural frequencies of FG sandwich beams.

3. Numerical results and discussion

A number of numerical examples are analyzed in this section to verify the accuracy of present study and investigate the critical buckling loads and natural frequencies of FG sandwich beams. Two types of FG sandwich beams are constituted by a mixture of isotropic ceramic (Al_2O_3) and metal (Al). The material properties of Al_2O_3 are: E_c=380 GPa, ν_c=0.3, ρ_c=3960 kg/m^3, and those of Al are: E_m=70 GPa, ν_m=0.3, ρ_m=2702 kg/m^3. Effects of the power-law index, span-to-depth ratio, skin-core-skin thickness ratios and boundary conditions on the buckling and vibration behaviours of the FG sandwich beams are discussed in details. For simplicity, the nondimensional natural frequency and critical buckling parameters are defined as:

$$
\bar{\omega} = \frac{\omega L^2}{h}\sqrt{\frac{\rho_m}{E_m}},\, \bar{N}_{cr} = N_{cr}\frac{12L^2}{E_m h^3} \tag{24}
$$

Firstly, the convergence of the present polynomial series solution is studied. FG sandwich beams (type A, 1-2-1) with span-to-depth ratio (L/h=5) and power-law index (p=1) are considered. This is carried out for the fundamental frequency and critical buckling loads with three boundary conditions. The present results are compared with those based on a polynomial quasi-3D theory [24] in Fig. 2. It can be seen that the solution of S-S boundary condition converges more quickly than C-F and C-C ones, and that the number of terms m=14 is sufficient to obtain an accurate solution. This number will be therefore used throughout the numerical examples.

In the next example, Tables 2-13 present the comparison of the natural frequencies and critical buckling loads of FG sandwich beams of type A with three boundary conditions. They are calculated for various values of the power-law index, seven values of skin-core-skin thickness ratios and compared with the solutions obtained from HSBT ([18]), TSDT ([17]) and quasi-3D theory ([24]). It is seen that the solutions obtained from the proposed theory are in excellent agreement with those obtained from [24]. Besides, various differences between the HSDTs and the present theory appeared for thick

FG sandwich beams. Furthermore, it can be seen from the tables that the results decrease with the increase of the power-law index. The lowest and highest values of natural frequency and critical buckling load correspond to the (1-0-1) and (1-8-1) sandwich beams. It is due to the fact that these beams correspond to the lowest and highest volume fractions of the ceramic phase. The effect of the span-to-depth ratio on the fundamental frequencies and critical buckling loads of S-S FG sandwich beams with $p = 5$ is plotted in Fig. 3. It is observed that the effect of transverse shear deformation is effectively significant in the region $L/h \leq 25$. (2-1-2) FG sandwich beams with S-S and C-C boundary conditions are chosen to investigate further effect of normal strain by comparing results with HSBT [18] (without normal strain) in Figs. 4 and 5. It can be seen that the deviation on the critical buckling loads between the present model and previous one [18] is bigger than that on the fundamental frequency. Moreover, it is also observed that the effect of normal strain through the quasi-3D theory is effectively significant for thick and C-C FG sandwich beams.

Finally, the natural frequencies and critical buckling loads of FG sandwich beams of type B are compared with those obtained from HSBT [18] in Tables 14-16. They are carried out for two values of skin-core-skin thickness ratios (1-2-1 and 2-2-1), different values of the power-law index and different boundary conditions. It can be seen again that by accounting the normal strain, the present theory provides the solution bigger than the HSBT [18]. The first three mode shapes of C-C sandwich beams with the power-law index p=2 is illustrated in Fig. 6. Due to small stretching deformation, the resulting mode shape is referred to as triply coupled mode, which are substantial involving axial, shear and flexure deformation.

4. Conclusions

An analytical solution for buckling and free vibration analysis of FG sandwich beams is proposed in this paper. The proposed theory with a higher-order variation of displacements accounts both normal and transverse shear strains. Analytical polynomial series solutions are derived for three types of FG sandwich beams with various boundary conditions. Effects of the boundary conditions, power-law index, span-to-depth ratio and skin-core-skin thickness ratios on the critical buckling loads and natural frequencies are discussed. The proposed theory is accurate and efficient in solving the free vibration and buckling behaviours of the FG sandwich beams.

Acknowledgements

The fourth author gratefully acknowledges research support fund by the National Research Foundation of Korea (NRF) funded by the Ministry of Education, Science and Technology through 2015R1A2A1A01007535

References

[1] A. Chakraborty, S. Gopalakrishnan, J. N. Reddy, A new beam finite element for the analysis of functionally graded materials, International Journal of Mechanical Sciences 45 (3) (2003) 519 – 539.

[2] X.-F. Li, A unified approach for analyzing static and dynamic behaviors of functionally graded Timoshenko and Euler-Bernoulli beams, Journal of Sound and Vibration 318 (4-5) (2008) 1210 – 1229.

[3] S.-R. Li, R. C. Batra, Relations between buckling loads of functionally graded Timoshenko and homogeneous Euler-Bernoulli beams, Composite Structures 95 (0) (2013) 5 – 9.

[4] T.-K. Nguyen, T. P. Vo, H.-T. Thai, Static and free vibration of axially loaded functionally graded beams based on the first-order shear deformation theory, Composites Part B: Engineering 55 (0) (2013) 147 – 157.

[5] K. Pradhan, S. Chakraverty, Free vibration of euler and timoshenko functionally graded beams by Rayleigh-ritz method, Composites Part B: Engineering 51 (0) (2013) 175 – 184.

[6] S. Sina, H. Navazi, H. Haddadpour, An analytical method for free vibration analysis of functionally graded beams, Materials and Design 30 (3) (2009) 741 – 747.

[7] M. Aydogdu, V. Taskin, Free vibration analysis of functionally graded beams with simply supported edges, Materials and Design 28 (2007) 1651–1656.

[8] S. Kapuria, M. Bhattacharyya, A. N. Kumar, Bending and free vibration response of layered functionally graded beams: A theoretical model and its experimental validation, Composite Structures 82 (3) (2008) 390 – 402.

[9] R. Kadoli, K. Akhtar, N. Ganesan, Static analysis of functionally graded beams using higher order shear deformation theory, Applied Mathematical Modelling 32 (12) (2008) 2509 – 2525.

[10] M. A. Benatta, I. Mechab, A. Tounsi, E. A. A. Bedia, Static analysis of functionally graded short beams including warping and shear deformation effects, Computational Materials Science 44 (2) (2008) 765 – 773.

[11] S. Ben-Oumrane, T. Abedlouahed, M. Ismail, B. B. Mohamed, M. Mustapha, A. B. E. Abbas, A theoretical analysis of flexional bending of Al/Al2O3 S-FGM thick beams, Computational Materials Science 44 (4) (2009) 1344 – 1350.

[12] X.-F. Li, B.-L. Wang, J.-C. Han, A higher-order theory for static and dynamic analyses of functionally graded beams, Archive of Applied Mechanics 80 (2010) 1197–1212, 10.1007/s00419-010-0435-6.

[13] A. M. Zenkour, M. N. M. Allam, M. Sobhy, Bending analysis of fg viscoelastic sandwich beams with elastic cores resting on Pasternaks elastic foundations, Acta Mechanica 212 (2010) 233–252.

[14] M. Simsek, Fundamental frequency analysis of functionally graded beams by using different higher-order beam theories, Nuclear Engineering and Design 240 (4) (2010) 697 – 705.

[15] H. T. Thai, T. P. Vo, Bending and free vibration of functionally graded beams using various higher-order shear deformation beam theories, International Journal of Mechanical Sciences 62 (1) (2012) 57–66.

[16] T. P. Vo, H.-T. Thai, T.-K. Nguyen, F. Inam, Static and vibration analysis of functionally graded beams using refined shear deformation theory, Meccanica 49 (1) (2014) 155–168.

[17] T. P. Vo, H.-T. Thai, T.-K. Nguyen, A. Maheri, J. Lee, Finite element model for vibration and buckling of functionally graded sandwich beams based on a refined shear deformation theory, Engineering Structures 64 (2014) 12 – 22.

[18] T.-K. Nguyen, T. T.-P. Nguyen, T. P. Vo, H.-T. Thai, Vibration and buckling analysis of functionally graded sandwich beams by a new higher-order shear deformation theory, Composites Part B: Engineering 76 (0) (2015) 273 – 285.

[19] T.-K. Nguyen, B.-D. Nguyen, A new higher-order shear deformation theory for static, buckling and free vibration analysis of functionally graded sandwich beams, Journal of Sandwich Structures and Materials, 2015, In Press.

[20] E. Carrera, G. Giunta, M. Petrolo, Beam structures: classical and advanced theories, John Wiley & Sons, 2011.

[21] G. Giunta, S. Belouettar, E. Carrera, Analysis of FGM Beams by Means of Classical and Advanced Theories, Mechanics of Advanced Materials and Structures 17 (8) (2010) 622–635.

[22] D. S. Mashat, E. Carrera, A. M. Zenkour, S. A. A. Khateeb, M. Filippi, Free vibration of FGM layered beams by various theories and finite elements, Composites Part B: Engineering 59 (0) (2014) 269 – 278.

[23] M. Filippi, E. Carrera, A. M. Zenkour, Static analyses of {FGM} beams by various theories and finite elements, Composites Part B: Engineering 72 (0) (2015) 1 – 9.

[24] T. P. Vo, H.-T. Thai, T.-K. Nguyen, F. Inam, J. Lee, A quasi-3d theory for vibration and buckling of functionally graded sandwich beams, Composite Structures 119 (0) (2015) 1 – 12.

[25] T. P. Vo, H.-T. Thai, T.-K. Nguyen, F. Inam, J. Lee, Static behaviour of functionally graded sandwich beams using a quasi-3d theory, Composites Part B: Engineering 68 (0) (2015) 59 – 74.

[26] J. L. Mantari, J. Yarasca, A simple and accurate generalized shear deformation theory for beams, Composite Structures 134 (2015) 593 – 601.

[27] J. L. Mantari, A refined theory with stretching effect for the dynamics analysis of advanced composites on elastic foundation, Mechanics of Materials 86 (2015) 31–43.

[28] J. L. Mantari, Refined and generalized hybrid type quasi-3D shear deformation theory for the bending analysis of functionally graded shells, Composites Part B: Engineering 83 (2015) 142–152.

[29] A. I. Osofero, T. P. Vo, T.-K. Nguyen, J. Lee, Analytical solution for vibration and buckling of functionally graded sandwich beams using various quasi-3d theories, Journal of Sandwich Structures and Materials, 2015, In Press.

Table 1: Kinematic boundary conditions.

BC	$x = 0$	$x = L$
S-S	$w = 0$, $w_z = 0$	$w = 0$, $w_z = 0$
C-F	$u = 0$, $w = 0$, θ_x=0, $w_{,x}$=0, w_z=0	
C-C	$u = 0$, $w = 0$, θ_x=0, $w_{,x}$=0, w_z=0	$u = 0$, $w = 0$, θ_x=0, $w_{,x}$=0, w_z=0

Table 2: Nondimensional fundamental frequency ($\bar{\omega}$) of S-S FG sandwich beams (type A, L/h=5).

p	Theory	1-0-1	2-1-2	2-1-1	1-1-1	2-2-1	1-2-1	1-8-1
0	Present	5.1620	5.1620	5.1620	5.1620	5.1620	5.1620	5.1620
	HSBT [18]	5.1528	5.1528	5.1528	5.1528	5.1528	5.1528	-
	TSBT [17]	5.1528	5.1528	5.1528	5.1528	5.1528	5.1528	5.1528
	Quasi-3D [24]	5.1618	5.1618	5.1618	5.1618	5.1618	5.1618	5.1618
0.5	Present	4.1329	4.2417	4.3037	4.3373	4.4143	4.4874	4.8504
	HSBT [18]	4.1254	4.2340	4.2943	4.3294	4.4045	4.4791	-
	TSBT [17]	4.1268	4.2351	4.2945	4.3303	4.4051	4.4798	4.8422
	Quasi-3D [24]	4.1344	4.2429	4.3041	4.3383	4.4146	4.4881	4.8511
1	Present	3.5804	3.7369	3.8318	3.8830	4.0018	4.1185	4.6883
	HSBT [18]	3.5736	3.7298	3.8206	3.8756	3.9911	4.1105	-
	TSBT [17]	3.5735	3.7298	3.8187	3.8755	3.9896	4.1105	4.6795
	Quasi-3D [24]	3.5803	3.7369	3.8301	3.8830	4.0005	4.1185	4.6884
2	Present	3.0739	3.2428	3.3685	3.4258	3.5848	3.7410	4.5229
	HSBT [18]	3.0682	3.2366	3.3546	3.4190	3.5719	3.7334	-
	TSBT [17]	3.0680	3.2365	3.3514	3.4190	3.5692	3.7334	4.5142
	Quasi-3D [24]	3.0737	3.2427	3.3656	3.4257	3.5825	3.7410	4.5231
5	Present	2.7497	2.8491	2.9955	3.0239	3.2122	3.3840	4.3587
	HSBT [18]	2.7450	2.8441	2.9790	3.0182	3.1966	3.3771	-
	TSBT [17]	2.7446	2.8439	2.9746	3.0181	3.1928	3.3771	4.3501
	Quasi-3D [24]	2.7493	2.8489	2.9912	3.0238	3.2087	3.3840	4.3589
10	Present	2.6982	2.7402	2.8886	2.8862	3.0797	3.2423	4.2862
	HSBT [18]	2.6936	2.7357	2.8716	2.8810	3.0630	3.2357	-
	TSBT [17]	2.6932	2.7355	2.8669	2.8808	3.0588	3.2356	4.2776
	Quasi-3D [24]	2.6978	2.7400	2.8839	2.8860	3.0757	3.2422	4.2864

Table 3: Nondimensional fundamental frequency ($\bar{\omega}$) of S-S FG sandwich beams (L/h=20, type A).

p	Theory	1-0-1	2-1-2	2-1-1	1-1-1	2-2-1	1-2-1	1-8-1
0	Present	5.4611	5.4611	5.4611	5.4611	5.4611	5.4611	5.4611
	HSBT [18]	5.4603	5.4603	5.4603	5.4603	5.4603	5.4603	-
	TSBT [17]	5.4603	5.4603	5.4603	5.4603	5.4603	5.4603	5.4603
	Quasi-3D [24]	5.4610	5.4610	5.4610	5.4610	5.4610	5.4610	5.4610
0.5	Present	4.3137	4.4284	4.4983	4.5321	4.6182	4.6979	5.1067
	HSBT [18]	4.3132	4.4278	4.4960	4.5315	4.6158	4.6972	-
	TSBT [17]	4.3148	4.4290	4.4970	4.5324	4.6170	4.6979	5.1067
	Quasi-3D [24]	4.3153	4.4296	4.4992	4.5330	4.6190	4.6985	5.1073
1	Present	3.7153	3.8774	3.9824	4.0334	4.1643	4.2896	4.9240
	HSBT [18]	3.7147	3.8768	3.9775	4.0328	4.1603	4.2889	-
	TSBT [17]	3.7147	3.8768	3.9774	4.0328	4.1602	4.2889	4.9233
	Quasi-3D [24]	3.7152	3.8773	3.9822	4.0333	4.1641	4.2895	4.9239
2	Present	3.1769	3.3471	3.4842	3.5395	3.7121	3.8775	4.7389
	HSBT [18]	3.1764	3.3465	3.4756	3.5389	3.7051	3.8769	-
	TSBT [17]	3.1764	3.3465	3.4754	3.5389	3.7049	3.8769	4.7382
	Quasi-3D [24]	3.1768	3.3469	3.4838	3.5394	3.7118	3.8774	4.7388
5	Present	2.8444	2.9315	3.0899	3.1116	3.3138	3.4927	4.5561
	HSBT [18]	2.8440	2.9311	3.0776	3.1111	3.3030	3.4921	-
	TSBT [17]	2.8439	2.9310	3.0773	3.1111	3.3028	3.4921	4.5554
	Quasi-3D [24]	2.8443	2.9314	3.0891	3.1115	3.3133	3.4926	4.5560
10	Present	2.8046	2.8192	2.9797	2.9666	3.1739	3.3412	4.4756
	HSBT [18]	2.8042	2.8188	2.9665	2.9662	3.1616	3.3406	-
	TSBT [17]	2.8041	2.8188	2.9662	2.9662	3.1613	3.3406	4.4749
	Quasi-3D [24]	2.8045	2.8191	2.9786	2.9665	3.1732	3.3411	4.4755

Table 4: Nondimensional fundamental frequency ($\bar{\omega}$) of C-F FG sandwich beams (L/h=5, type A).

p	Theory	1-0-1	2-1-2	2-1-1	1-1-1	2-2-1	1-2-1	1-8-1
0	Present	1.9053	1.9053	1.9053	1.9053	1.9053	1.9053	1.9053
	HSBT [18]	1.8953	1.8953	1.8953	1.8953	1.8953	1.8953	-
	TSBT [17]	1.8952	1.8952	1.8952	1.8952	1.8952	1.8952	1.8952
	Quasi-3D [24]	1.9055	1.9055	1.9055	1.9055	1.9055	1.9055	1.9055
0.5	Present	1.5142	1.5543	1.5779	1.5901	1.6193	1.6467	1.7853
	HSBT [18]	1.5064	1.5463	1.5693	1.5819	1.6104	1.6383	-
	TSBT [17]	1.5069	1.5466	1.5696	1.5821	1.6108	1.6384	1.7764
	Quasi-3D [24]	1.5152	1.5551	1.5787	1.5908	1.6200	1.6474	1.7859
1	Present	1.3077	1.3648	1.4005	1.4189	1.4636	1.5071	1.7232
	HSBT [18]	1.3008	1.3576	1.3919	1.4115	1.4550	1.4993	-
	TSBT [17]	1.3007	1.3575	1.3918	1.4115	1.4549	1.4992	1.7145
	Quasi-3D [24]	1.3081	1.3652	1.4008	1.4193	1.4640	1.5075	1.7235
2	Present	1.1204	1.1810	1.2278	1.2483	1.3074	1.3653	1.6601
	HSBT [18]	1.1143	1.1747	1.2189	1.2416	1.2987	1.3582	-
	TSBT [17]	1.1143	1.1746	1.2188	1.2416	1.2986	1.3582	1.6518
	Quasi-3D [24]	1.1208	1.1815	1.2282	1.2488	1.3079	1.3658	1.6605
5	Present	1.0028	1.0361	1.0902	1.0997	1.1691	1.2323	1.5976
	HSBT [18]	0.9974	1.0304	1.0807	1.0936	1.1598	1.2258	-
	TSBT [17]	0.9973	1.0303	1.0806	1.0935	1.1597	1.2257	1.5897
	Quasi-3D [24]	1.0030	1.0365	1.0904	1.1002	1.1695	1.2329	1.5981
10	Present	0.9865	0.9965	1.0513	1.0491	1.1203	1.1798	1.5701
	HSBT [18]	0.9813	0.9910	1.0417	1.0432	1.1106	1.1734	-
	TSBT [17]	0.9812	0.9909	1.0416	1.0431	1.1106	1.1734	1.5624
	Quasi-3D [24]	0.9867	0.9969	1.0514	1.0495	1.1206	1.1804	1.5706

Table 5: Nondimensional fundamental frequency ($\bar{\omega}$) of C-F FG sandwich beams (L/h=20, type A).

p	Theory	1-0-1	2-1-2	2-1-1	1-1-1	2-2-1	1-2-1	1-8-1
0	Present	1.9530	1.9530	1.9530	1.9530	1.9530	1.9530	1.9530
	HSBT [18]	1.9496	1.9496	1.9496	1.9496	1.9496	1.9496	-
	TSBT [17]	1.9496	1.9496	1.9496	1.9496	1.9496	1.9496	1.9496
	Quasi-3D [24]	1.9527	1.9527	1.9527	1.9527	1.9527	1.9527	1.9527
0.5	Present	1.5422	1.5832	1.6081	1.6203	1.6511	1.6796	1.8260
	HSBT [18]	1.5392	1.5801	1.6045	1.6171	1.6473	1.6764	-
	TSBT [17]	1.5397	1.5805	1.6048	1.6175	1.6477	1.6766	1.8229
	Quasi-3D [24]	1.5423	1.5831	1.6081	1.6201	1.6509	1.6794	1.8259
1	Present	1.3281	1.3860	1.4235	1.4418	1.4886	1.5335	1.7606
	HSBT [18]	1.3253	1.3831	1.4191	1.4388	1.4844	1.5304	-
	TSBT [17]	1.3253	1.3831	1.4191	1.4388	1.4844	1.5304	1.7573
	Quasi-3D [24]	1.3275	1.3855	1.4230	1.4413	1.4881	1.5329	1.7602
2	Present	1.1355	1.1964	1.2453	1.2651	1.3268	1.3860	1.6943
	HSBT [18]	1.1330	1.1937	1.2398	1.2623	1.3217	1.3831	-
	TSBT [17]	1.1330	1.1937	1.2398	1.2623	1.3217	1.3831	1.6911
	Quasi-3D [24]	1.1351	1.1958	1.2447	1.2646	1.3262	1.3855	1.6938
5	Present	1.0167	1.0478	1.1042	1.1122	1.1843	1.2484	1.6289
	HSBT [18]	1.0145	1.0454	1.0977	1.1096	1.1781	1.2456	-
	TSBT [17]	1.0145	1.0453	1.0977	1.1096	1.1781	1.2456	1.6257
	Quasi-3D [24]	1.0163	1.0473	1.1036	1.1116	1.1837	1.2478	1.6284
10	Present	1.0025	1.0077	1.0648	1.0604	1.1342	1.1943	1.6001
	HSBT [18]	1.0005	1.0053	1.0581	1.0578	1.1276	1.1915	-
	TSBT [17]	1.0005	1.0053	1.0581	1.0578	1.1276	1.1915	1.5969
	Quasi-3D [24]	1.0022	1.0072	1.0641	1.0598	1.1336	1.1937	1.5995

Table 6: Nondimensional fundamental frequency ($\bar{\omega}$) of C-C FG sandwich beams (L/h=5, type A).

p	Theory	1-0-1	2-1-2	2-1-1	1-1-1	2-2-1	1-2-1	1-8-1
0	Present	10.1790	10.1790	10.1790	10.1790	10.1790	10.1790	10.1790
	HSBT [18]	10.0726	10.0726	10.0726	10.0726	10.0726	10.0726	-
	TSBT [17]	10.0678	10.0678	10.0678	10.0678	10.0678	10.0678	10.0678
	Quasi-3D [24]	10.1851	10.1851	10.1851	10.1851	10.1851	10.1851	10.1851
0.5	Present	8.4503	8.6657	8.7633	8.8381	8.9629	9.0924	9.6747
	HSBT [18]	8.3606	8.5736	8.6688	8.7442	8.8654	8.9969	-
	TSBT [17]	8.3600	8.5720	8.6673	8.7423	8.8648	8.9942	9.5731
	Quasi-3D [24]	8.4635	8.6780	8.7755	8.8498	8.9743	9.1036	9.6857
1	Present	7.4534	7.7769	7.9343	8.0504	8.2521	8.4653	9.4078
	HSBT [18]	7.3707	7.6910	7.8428	7.9623	8.1593	8.3747	-
	TSBT [17]	7.3661	7.6865	7.8390	7.9580	8.1554	8.3705	9.3076
	Quasi-3D [24]	7.4611	7.7854	7.9431	8.0595	8.2615	8.4752	9.4174
2	Present	6.4888	6.8660	7.0836	7.2237	7.5048	7.8008	9.1307
	HSBT [18]	6.4139	6.7867	6.9939	7.1412	7.4138	7.7149	-
	TSBT [17]	6.4095	6.7826	6.9908	7.1373	7.4105	7.7114	9.0343
	Quasi-3D [24]	6.4952	6.8740	7.0920	7.2328	7.5143	7.8114	9.1415
5	Present	5.7977	6.1060	6.3650	6.4701	6.8126	7.1550	8.8536
	HSBT [18]	5.7315	6.0335	6.2765	6.3925	6.7216	7.0723	-
	TSBT [17]	5.7264	6.0293	6.2737	6.3889	6.7188	7.0691	8.7605
	Quasi-3D [24]	5.8016	6.1124	6.3718	6.4780	6.8210	7.1652	8.8653
10	Present	5.6049	5.8793	6.1424	6.2028	6.5577	6.8934	8.7311
	HSBT [18]	5.5429	5.8104	6.0555	6.1278	6.4668	6.8119	-
	TSBT [17]	5.5375	5.8059	6.0527	6.1240	6.4641	6.8087	8.6391
	Quasi-3D [24]	5.6074	5.8848	6.1485	6.2099	6.5654	6.9030	8.7430

Table 7: Nondimensional fundamental frequency ($\bar{\omega}$) of C-C FG sandwich beams (L/h=20, type A).

p	Theory	1-0-1	2-1-2	2-1-1	1-1-1	2-2-1	1-2-1	1-8-1
0	Present	12.2756	12.2756	12.2756	12.2756	12.2756	12.2756	12.2756
	HSBT [18]	12.2243	12.2243	12.2243	12.2243	12.2243	12.2243	-
	TSBT [17]	12.2228	12.2228	12.2228	12.2228	12.2228	12.2228	12.2228
	Quasi-3D [24]	12.2660	12.2660	12.2660	12.2660	12.2660	12.2660	12.2660
0.5	Present	9.7353	9.9933	10.1471	10.2246	10.4148	10.5924	11.4949
	HSBT [18]	9.6916	9.9484	10.0985	10.1788	10.3647	10.5455	-
	TSBT [17]	9.6942	9.9501	10.1001	10.1800	10.3668	10.5460	11.4459
	Quasi-3D [24]	9.7297	9.9865	10.1403	10.2172	10.4072	10.5842	11.4867
1	Present	8.3998	8.7663	8.9984	9.1158	9.4057	9.6866	11.0916
	HSBT [18]	8.3601	8.7248	8.9479	9.0729	9.3555	9.6419	-
	TSBT [17]	8.3594	8.7241	8.9474	9.0722	9.3550	9.6411	11.0421
	Quasi-3D [24]	8.3908	8.7569	8.9893	9.1061	9.3964	9.6768	11.0815
2	Present	7.1920	7.5799	7.8836	8.0128	8.3964	8.7690	10.6820
	HSBT [18]	7.1568	7.5422	7.8293	7.9732	8.3431	8.7268	-
	TSBT [17]	7.1563	7.5417	7.8293	7.9727	8.3430	8.7262	10.6336
	Quasi-3D [24]	7.1839	7.5711	7.8753	8.0035	8.3877	8.7593	10.6719
5	Present	6.4381	6.6461	6.9970	7.0536	7.5037	7.9092	10.2771
	HSBT [18]	6.4071	6.6121	6.9387	7.0174	7.4459	7.8696	-
	TSBT [17]	6.4064	6.6116	6.9389	7.0170	7.4461	7.8692	10.2298
	Quasi-3D [24]	6.4308	6.6379	6.9891	7.0451	7.4955	7.9000	10.2669
10	Present	6.3385	6.3920	6.7473	6.7277	7.1889	7.5700	10.0987
	HSBT [18]	6.3094	6.3595	6.6887	6.6928	7.1293	7.5315	-
	TSBT [17]	6.3086	6.3590	6.6889	6.6924	7.1296	7.5311	10.0519
	Quasi-3D [24]	6.3319	6.3841	6.7395	6.7194	7.1809	7.5609	10.0884

Table 8: Nondimensional critical buckling load ($\bar{N}_{cr}$) of S-S FG sandwich beams (L/h=5, type A).

p	Theory	1-0-1	2-1-2	2-1-1	1-1-1	2-2-1	1-2-1	1-8-1
0	Present	49.5970	49.5970	49.5970	49.5970	49.5970	49.5970	49.5970
	HSBT [18]	48.5964	48.5964	48.5964	48.5964	48.5964	48.5964	-
	TSBT [17]	48.5959	48.5959	48.5959	48.5959	48.5959	48.5959	48.5959
	Quasi-3D [24]	49.5906	49.5906	49.5906	49.5906	49.5906	49.5906	49.5906
0.5	Present	28.4407	30.6650	31.7459	32.5547	33.9720	35.5032	42.8623
	HSBT [18]	27.8380	30.0146	31.0577	31.8650	33.2336	34.7546	-
	TSBT [17]	27.8574	30.0301	31.0728	31.8784	33.2536	34.7653	41.9897
	Quasi-3D [24]	28.4624	30.6825	31.7627	32.5699	33.9858	35.5156	42.8751
1	Present	20.0899	22.7061	24.0833	25.1060	26.9747	29.0723	39.6116
	HSBT [18]	19.6541	22.2121	23.5250	24.5602	26.3611	28.4440	-
	TSBT [17]	19.6525	22.2108	23.5246	24.5596	26.3611	28.4447	38.7838
	Quasi-3D [24]	20.7425	22.7065	24.0838	25.1075	26.9764	29.0755	39.6144
2	Present	13.8852	16.2761	17.7748	18.7756	20.8863	23.3002	36.4626
	HSBT [18]	13.5820	15.9167	17.3254	18.3596	20.3751	22.7859	-
	TSBT [17]	13.5801	15.9152	17.3249	18.3587	20.3750	22.7863	35.6914
	Quasi-3D [24]	13.8839	16.2761	17.7742	18.7772	20.8879	23.3042	36.4677
5	Present	10.3708	11.9320	13.3963	14.0352	16.1613	18.5058	33.4891
	HSBT [18]	10.1488	11.6697	13.0279	13.7226	15.7313	18.0915	-
	TSBT [17]	10.1460	11.6676	13.0270	13.7212	15.7307	18.0914	32.7725
	Quasi-3D [24]	10.3673	11.9301	13.3924	14.0353	16.1605	18.5092	33.4958
10	Present	9.6573	10.7715	12.1790	12.5402	14.6018	16.7550	32.2197
	HSBT [18]	9.4543	10.5370	11.8380	12.2621	14.2002	16.3789	-
	TSBT [17]	9.4515	10.5348	11.8370	12.2605	14.1995	16.3783	31.5265
	Quasi-3D [24]	9.6535	10.7689	12.1737	12.5393	14.5994	16.7574	32.2264

Table 9: Nondimensional critical buckling load ($\bar{N}_{cr}$) of S-S FG sandwich beams (L/h=20, type A).

p	Theory	1-0-1	2-1-2	2-1-1	1-1-1	2-2-1	1-2-1	1-8-1
0	Present	53.3175	53.3175	53.3175	53.3175	53.3175	53.3175	53.3175
	HSBT [18]	53.2364	53.2364	53.2364	53.2364	53.2364	53.2364	-
	TSBT [17]	53.2364	53.2364	53.2364	53.2364	53.2364	53.2364	53.2364
	Quasi-3D [24]	53.3145	53.3145	53.3145	53.3145	53.3145	53.3145	53.3145
0.5	Present	29.7410	32.0853	33.2971	34.1242	35.7026	37.3626	45.6315
	HSBT [19]	29.6965	32.0368	33.2217	34.0722	35.6202	37.3054	-
	TSBT [17]	29.7175	32.2629	33.2376	34.0862	35.6405	37.3159	45.5742
	Quasi-3D [24]	29.7626	32.1022	33.3127	34.1380	35.7149	41.8227	45.6424
1	Present	20.7541	23.4584	24.9715	26.0001	28.0424	30.2785	41.9655
	HSBT [18]	20.7213	23.4212	24.8793	25.9588	27.9537	30.2306	-
	TSBT [17]	20.7212	23.4211	24.8796	25.9588	27.9540	30.2307	41.9004
	Quasi-3D [24]	20.7530	23.4572	24.9697	25.9989	28.0412	30.2774	41.9639
2	Present	14.2199	16.6317	18.2521	19.2309	21.5001	24.0284	38.4431
	HSBT [18]	14.1974	16.6051	18.1400	19.2000	21.3923	23.9899	-
	TSBT [17]	14.1973	16.6050	18.1404	19.3116	21.3927	23.9900	38.3831
	Quasi-3D [24]	14.2190	16.6307	18.2493	19.2299	21.4986	24.0276	38.4419
5	Present	10.6341	12.1078	13.6771	14.2515	16.5100	18.9180	35.1408
	HSBT [18]	10.6176	12.0886	13.5520	14.2285	16.3829	18.8874	-
	TSBT [17]	10.6171	12.0883	13.5523	14.2284	16.3834	18.8874	35.0856
	Quasi-3D [24]	10.6330	12.1068	13.6717	14.2505	16.5069	18.9172	35.1400
10	Present	10.0003	10.9246	12.4320	12.7023	14.8851	17.0723	33.7379
	HSBT [18]	9.9850	10.9075	12.3081	12.6820	14.7520	17.0445	-
	TSBT [17]	9.9847	10.9075	12.3084	12.6819	14.7525	17.0443	33.6843
	Quasi-3D [24]	9.9995	10.9239	12.4256	12.7014	14.8807	17.0712	33.7367

Table 10: Nondimensional critical buckling load ($\bar{N}_{cr}$) of C-C FG sandwich beams (L/h=5, type A).

p	Theory	1-0-1	2-1-2	2-1-1	1-1-1	2-2-1	1-2-1	1-8-1
0	Present	160.3064	160.3064	160.3064	160.3064	160.3064	160.3064	160.3064
	HSBT [18]	152.1588	152.1588	152.1588	152.1588	152.1588	152.1588	-
	TSBT [17]	152.1470	152.1470	152.1470	152.1470	152.1470	152.1470	152.1470
	Quasi-3D [24]	160.2780	160.2780	160.2780	160.2780	160.2780	160.2780	160.2780
0.5	Present	98.3648	105.8972	108.9555	111.8943	116.0009	120.7931	141.7160
	HSBT [18]	92.8202	99.9361	102.8605	105.6331	109.5284	114.1312	-
	TSBT [17]	92.8833	99.9860	102.9120	105.6790	109.6030	114.1710	134.2870
	Quasi-3D [24]	98.4559	105.9750	109.0360	111.9680	116.0700	120.8630	141.7880
1	Present	71.7633	81.0819	85.1883	89.0595	94.7381	101.5703	132.5067
	HSBT [18]	67.5184	76.2801	80.1730	83.8267	89.2223	95.7230	-
	TSBT [17]	67.4983	76.2634	80.1670	83.8177	89.2208	95.7287	125.3860
	Quasi-3D [24]	71.7654	81.0936	85.2092	89.0834	94.7675	101.6130	132.5510
2	Present	50.8264	59.9292	64.5957	68.6517	75.3511	83.5671	123.4142
	HSBT [18]	47.7247	56.2259	60.6127	64.4352	70.7590	78.5570	-
	TSBT [17]	47.7010	56.2057	60.6056	64.4229	70.7563	78.5608	116.6580
	Quasi-3D [24]	50.8183	59.9354	64.6133	68.6743	75.3818	83.6159	123.4770
5	Present	37.8590	44.8607	49.5296	52.6318	59.6057	68.0098	114.6926
	HSBT [18]	35.5811	42.0298	46.3852	49.2949	55.8338	63.7847	-
	TSBT [17]	35.5493	42.0033	46.3743	49.2763	55.8271	63.7824	108.2970
	Quasi-3D [24]	37.8295	44.8488	49.5325	52.6395	59.6248	68.0510	114.77
10	Present	34.3176	40.5751	45.0701	47.3821	54.2081	62.1634	110.9318
	HSBT [18]	32.3345	38.0239	42.2062	44.3593	50.7406	58.2532	-
	TSBT [17]	32.3019	37.9944	42.1935	44.3374	50.7315	58.2461	104.6920
	Quasi-3D [24]	34.2824	40.5544	45.0660	47.3804	54.2193	62.1959	111.0120

Table 11: Nondimensional critical buckling load ($\bar{N}_{cr}$) of C-C FG sandwich beams (L/h=20, type A).

p	Theory	1-0-1	2-1-2	2-1-1	1-1-1	2-2-1	1-2-1	1-8-1
0	Present	210.7774	210.7774	210.7774	210.7774	210.7774	210.7774	210.7774
	HSBT [18]	208.9515	208.9515	208.9515	208.9515	208.9515	208.9515	-
	TSBT [17]	208.9510	208.9510	208.9510	208.9510	208.9510	208.9510	208.9510
	Quasi-3D [24]	210.7420	210.7420	210.7420	210.7420	210.7420	210.7420	210.7420
0.5	Present	118.3095	127.6190	132.3616	135.6735	141.8619	148.4165	180.7913
	HSBT [18]	117.2200	126.4422	131.0594	134.4255	140.4622	147.0614	-
	TSBT [17]	117.3030	126.5080	131.1240	134.4810	140.5450	147.1040	179.2350
	Quasi-3D [24]	118.3530	127.6410	132.3830	135.6840	141.8690	148.4130	180.8010
1	Present	82.7901	93.5770	99.5203	103.6595	111.6956	120.5619	166.4508
	HSBT [18]	81.9944	92.6754	98.3839	102.6655	110.4792	119.4215	-
	TSBT [17]	81.9927	92.6741	98.3880	102.6650	110.4830	119.4220	164.9490
	Quasi-3D [24]	82.7434	93.5248	99.4730	103.6060	111.6480	120.5090	166.4060
2	Present	56.8386	66.5147	72.8955	76.8684	85.8241	95.8941	152.6477
	HSBT [18]	56.2793	65.8505	71.8837	76.1030	84.7230	94.9558	-
	TSBT [17]	56.2773	65.8489	71.8900	76.1020	84.7291	94.9563	151.2500
	Quasi-3D [24]	56.7986	66.4664	72.8506	76.8166	85.7783	95.8403	152.6000
5	Present	42.4914	48.5016	54.6876	57.0817	66.0121	75.6538	139.6866
	HSBT [18]	42.0814	48.0095	53.7751	56.4973	64.9930	74.8903	-
	TSBT [17]	42.0775	48.0070	53.7820	56.4958	65.0007	74.8903	138.3880
	Quasi-3D [24]	42.4596	48.4588	54.6418	57.0343	65.9671	75.6019	139.6370
10	Present	39.8676	43.7664	49.7084	50.9062	59.5406	68.3252	134.1743
	HSBT [18]	39.4962	43.3252	48.8443	50.3827	58.5529	67.6281	-
	TSBT [17]	39.4930	43.3233	48.8510	50.3811	58.5607	67.6270	132.9170
	Quasi-3D [24]	39.8436	43.7273	49.6622	50.8611	59.4944	68.2737	134.1220

Table 12: Nondimensional critical buckling load ($\bar{N}_{cr}$) of C-F FG sandwich beams (L/h=5, type A).

p	Theory	1-0-1	2-1-2	2-1-1	1-1-1	2-2-1	1-2-1	1-8-1
0	Present	13.1138	13.1138	13.1138	13.1138	13.1138	13.1138	13.1138
	HSBT [18]	13.0595	13.0595	13.0595	13.0595	13.0595	13.0595	-
	TSBT [17]	13.0594	13.0594	13.0594	13.0594	13.0594	13.0594	13.0594
	Quasi-3D [24]	13.1224	13.1224	13.1224	13.1224	13.1224	13.1224	13.1224
0.5	Present	7.3567	7.9357	8.2309	8.4366	8.8217	9.2289	11.2428
	HSBT [18]	7.3263	7.9026	8.1912	8.4016	8.7789	9.1913	-
	TSBT [17]	7.3314	7.9068	8.1951	8.4051	8.7839	9.1940	11.2021
	Quasi-3D [24]	7.3700	7.9482	8.2431	8.4486	8.8334	9.2404	11.2557
1	Present	5.1480	5.8182	6.1882	6.4447	6.9446	7.4948	10.3484
	HSBT [18]	5.1246	5.7922	6.1490	6.4166	6.9050	7.4638	-
	TSBT [17]	5.1245	5.7921	6.1490	6.4166	6.9050	7.4639	10.3093
	Quasi-3D [24]	5.1533	5.8244	6.1944	6.4516	6.9518	7.5028	10.3581
2	Present	3.5350	4.1359	4.5331	4.7789	5.3359	5.9601	9.4872
	HSBT [18]	3.5175	4.1157	4.4927	4.7564	5.2952	5.9347	-
	TSBT [17]	3.5173	4.1156	4.4927	4.7564	5.2952	5.9348	9.4531
	Quasi-3D [24]	3.5387	4.1408	4.5376	4.7847	5.3419	5.9674	9.4974
5	Present	2.6435	3.0170	3.4021	3.5501	4.1053	4.7028	8.6791
	HSBT [18]	2.6301	3.0006	3.3609	3.5311	4.0621	4.6806	-
	TSBT [17]	2.6298	3.0004	3.3609	3.5310	4.0620	4.6806	8.6493
	Quasi-3D [24]	2.6458	3.0203	3.4046	3.5542	4.1095	4.7088	8.6897
10	Present	2.4803	2.7226	3.0928	3.1665	3.7035	4.2480	8.3359
	HSBT [18]	2.4685	2.7078	3.0528	3.1489	3.6596	4.2268	-
	TSBT [17]	2.4683	2.7077	3.0527	3.1488	3.6595	4.2267	8.3073
	Quasi-3D [24]	2.4823	2.7257	3.0946	3.1702	3.7068	4.2533	8.3463

Table 13: Nondimensional critical buckling load ($\bar{N}_{cr}$) of C-F FG sandwich beams (L/h=20, type A).

p	Theory	1-0-1	2-1-2	2-1-1	1-1-1	2-2-1	1-2-1	1-8-1
0	Present	13.3993	13.3993	13.3993	13.3993	13.3993	13.3993	13.3993
	HSBT [18]	13.3730	13.3730	13.3730	13.3730	13.3730	13.3730	-
	TSBT [17]	13.3730	13.3730	13.3730	13.3730	13.3730	13.3730	13.3730
	Quasi-3D [24]	13.3981	13.3981	13.3981	13.3981	13.3981	13.3981	13.3981
0.5	Present	7.4649	8.0536	8.3585	8.5660	8.9631	9.3806	11.4625
	HSBT [18]	7.4490	8.0363	8.3345	8.5477	8.9372	9.3607	-
	TSBT [17]	7.4543	8.0405	8.3385	8.5512	8.9422	9.3634	11.4424
	Quasi-3D [24]	7.4689	8.0563	8.3609	8.5679	8.9647	9.3815	11.4642
1	Present	5.2067	5.8851	6.2654	6.5234	7.0367	7.5986	10.5393
	HSBT [18]	5.1944	5.8713	6.2378	6.5083	7.0096	7.5815	-
	TSBT [17]	5.1944	5.8713	6.2378	6.5083	7.0096	7.5815	10.5174
	Quasi-3D [24]	5.2050	5.8832	6.2633	6.5214	7.0346	7.5965	10.5375
2	Present	3.5662	4.1708	4.5775	4.8230	5.3927	6.0278	9.6526
	HSBT [18]	3.5574	4.1603	4.5457	4.8110	5.3615	6.0134	-
	TSBT [17]	3.5574	4.1603	4.5457	4.8110	5.3615	6.0134	9.6321
	Quasi-3D [24]	3.5648	4.1690	4.5753	4.8211	5.3906	6.0257	9.6507
5	Present	2.6670	3.0356	3.4291	3.5732	4.1396	4.7443	8.8217
	HSBT [18]	2.6606	3.0276	3.3948	3.5637	4.1042	4.7323	-
	TSBT [17]	2.6605	3.0275	3.3948	3.5637	4.1043	4.7323	8.8025
	Quasi-3D [24]	2.6659	3.0341	3.4266	3.5714	4.1373	4.7423	8.8196
10	Present	2.5090	2.7389	3.1168	3.1845	3.7318	4.2809	8.4688
	HSBT [18]	2.5033	2.7317	3.0831	3.1759	3.6952	4.2698	-
	TSBT [17]	2.5032	2.7317	3.0832	3.1759	3.6952	4.2698	8.4500
	Quasi-3D [24]	2.5082	2.7376	3.1142	3.1829	3.7293	4.2789	8.4666

Table 14: Nondimensional fundamental frequency of FG sandwich beams with various boundary conditions (type B).

Scheme	L/h	BC	Theory	p					
				0	0.5	1	2	5	10
1-2-1	5	S-S	Present	4.0996	3.8438	3.7172	3.6119	3.5513	3.5413
			HSBT [18]	4.0691	3.7976	3.6636	3.5530	3.4914	3.4830
		C-C	Present	8.4529	7.8924	7.5904	7.2898	7.0032	6.8757
			HSBT [18]	8.3282	7.7553	7.4487	7.1485	6.8702	6.7543
		C-F	Present	1.5001	1.4076	1.3627	1.3273	1.3113	1.3118
			HSBT [18]	1.4840	1.3865	1.3393	1.3022	1.2857	1.2867
	20	S-S	Present	4.2711	4.0143	3.8923	3.8003	3.7708	3.7831
			HSBT [18]	4.2445	3.9695	3.8387	3.7402	3.7081	3.7214
		C-C	Present	9.6404	9.0524	8.7701	8.5509	8.4627	8.4755
			HSBT [18]	9.5451	8.9243	8.6264	8.3959	8.3047	8.3205
		C-F	Present	1.5264	1.4344	1.3907	1.3580	1.3478	1.3525
			HSBT [18]	1.5145	1.4165	1.3700	1.3350	1.3241	1.3292
2-2-1	5	S-S	Present	3.7142	3.6270	3.5885	3.5589	3.5411	3.5352
			HSBT [18]	3.6624	3.5692	3.5292	3.5002	3.4858	3.4830
		C-C	Present	7.7159	7.4082	7.2306	7.0320	6.8091	6.7045
			HSBT [18]	7.5709	7.2636	7.0901	6.9040	6.8998	6.5941
		C-F	Present	1.3571	1.3297	1.3191	1.3135	1.3144	1.3160
			HSBT [18]	1.3344	1.3050	1.2939	1.2884	1.2903	1.2930
	20	S-S	Present	3.8647	3.7990	3.7784	3.7756	3.7966	3.8110
			HSBT [18]	3.8136	3.7406	3.7177	3.7144	3.7380	3.7552
		C-C	Present	8.7233	8.5588	8.4999	8.4757	8.4970	8.5157
			HSBT [18]	8.5832	8.4064	8.3442	8.3205	8.3488	8.3738
		C-F	Present	1.3807	1.3573	1.3501	1.3495	1.3576	1.3630
			HSBT [18]	1.3607	1.3350	1.3271	1.3263	1.3353	1.3418

Table 15: Nondimensional critical buckling load of FG sandwich beams with various boundary conditions (type B).

Scheme	L/h	BC	Theory	p					
				0	0.5	1	2	5	10
1-2-1	5	S-S	Present	28.7884	23.8554	21.6374	19.7957	18.5212	18.1329
			HSBT [18]	27.9314	22.9869	20.7762	18.9588	17.7320	17.3775
		C-C		100.5883	82.4783	73.9348	66.1308	59.2628	56.4049
			HSBT [18]	94.6117	77.5129	69.4877	62.2249	55.9446	53.3734
		C-F		7.4344	6.1836	5.6304	5.1884	4.9228	4.8658
			HSBT [18]	7.3149	6.0286	5.4629	5.0154	4.7534	4.7024
	20	S-S		30.0168	24.9914	22.7796	21.0343	20.0386	19.8622
			HSBT [18]	29.6120	24.4140	22.1386	20.3581	19.3639	19.2058
		C-C		119.4172	99.2742	90.3696	83.2627	79.0045	78.0989
			HSBT [18]	117.0384	96.4573	87.4069	80.2465	76.0539	75.2379
		C-F		7.5312	6.2702	5.7160	5.2800	5.0345	4.9934
			HSBT [18]	7.4254	6.1225	5.5529	5.1084	4.8634	4.8269
2-2-1	5	S-S		22.4065	20.3457	19.4156	18.6007	17.9128	17.6221
			HSBT [18]	21.5207	19.4909	18.5897	17.8178	17.1942	16.9422
		C-C		79.0342	69.4910	64.6563	59.7538	54.7871	52.5943
			HSBT [18]	74.0960	65.2766	60.8501	56.4008	51.9303	49.9605
		C-F		5.7754	5.2959	5.0939	4.9372	4.8346	4.7977
			HSBT [18]	5.6078	5.1228	4.9221	4.7709	4.6809	4.6533
	20	S-S		23.3038	21.4284	20.6576	20.0894	19.7694	19.6701
			HSBT [18]	22.6714	20.7578	19.9839	19.4292	19.1504	19.0848
		C-C		92.7010	84.9897	81.7465	79.2375	77.6098	77.0306
			HSBT [18]	89.7255	81.9647	78.7529	76.3344	74.8949	74.4533
		C-F		5.8444	5.3767	5.1857	5.0468	4.9722	4.9504
			HSBT [18]	5.6831	5.2064	5.0148	4.8794	4.8150	4.8016

Table 16: The first three nondimensional frequencies of FG sandwich beams (type B) with C-C boundary condition.

Mode	Type	L/h	Theory	p					
				0	0.5	1	2	5	10
1	1-2-1	5	Present	8.4529	7.8924	7.5904	7.2898	7.0032	6.8757
			HSBT [18]	8.3282	7.7553	7.4487	7.1485	6.8702	6.7543
		20	Present	9.6404	9.0524	8.7701	8.5509	8.4627	8.4755
			HSBT [18]	9.5451	8.9243	8.6264	8.3959	8.3047	8.3205
	2-2-1	5	Present	7.7159	7.4082	7.2306	7.0320	6.8091	6.7045
			HSBT [18]	7.5709	7.2636	7.0901	6.9040	6.8998	6.5941
		20	Present	8.7233	8.5588	8.4999	8.4757	8.4970	8.5157
			HSBT [18]	8.5832	8.4064	8.3442	8.3205	8.3488	8.3738
2	1-2-1	5	Present	20.1538	18.7348	17.9231	17.0413	16.0837	15.6231
			HSBT [18]	19.8886	18.4463	17.6290	16.7552	15.8266	15.3878
		20	Present	26.2039	24.5867	23.7980	23.1611	22.8406	22.8197
			HSBT [18]	25.9323	24.2300	23.4015	22.7371	22.4123	22.4014
	2-2-1	5	Present	18.4986	17.4894	16.8786	16.1729	15.3753	15.0105
			HSBT [18]	18.1865	17.1905	16.5950	15.9164	15.1574	14.8131
		20	Present	23.7284	23.2234	23.0169	22.8833	22.8435	22.8431
			HSBT [18]	23.3403	22.8045	22.5913	22.4619	22.4443	22.4623
3	1-2-1	5	Present	34.4230	31.9202	30.4476	28.7917	26.9294	26.0255
			HSBT [18]	34.0624	31.5260	30.0458	28.4068	26.5927	25.7241
		20	Present	50.4317	47.2723	45.7039	44.3844	43.5884	43.4278
			HSBT [18]	49.8846	46.5716	44.9326	43.5667	42.7705	42.6332
	2-2-1	5	Present	31.7174	29.7117	28.4955	27.0964	25.5375	24.8362
			HSBT [18]	31.2772	29.2997	28.1131	26.7610	25.2645	24.5968
		20	Present	45.7032	44.5962	44.0940	43.6868	43.4002	43.2918
			HSBT [18]	44.9445	43.7848	43.2741	42.8808	42.6431	42.5723

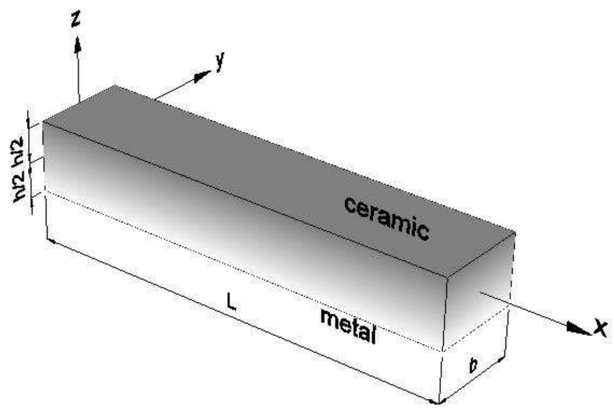

(a) FG sandwich beams with length L and section $b \times h$

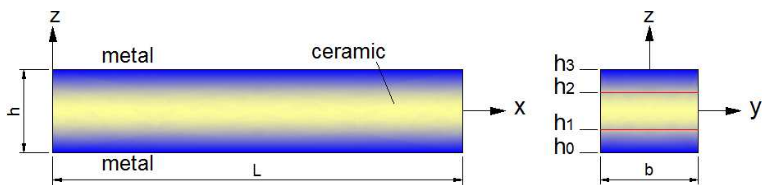

(b) Type A

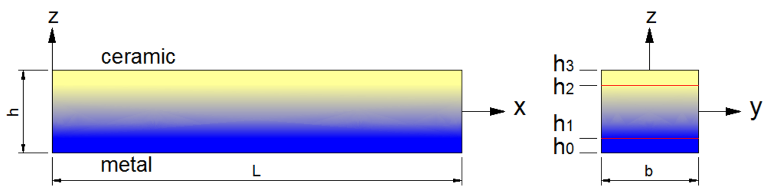

(c) Type B

Figure 1: Geometry of FG sandwich beams.

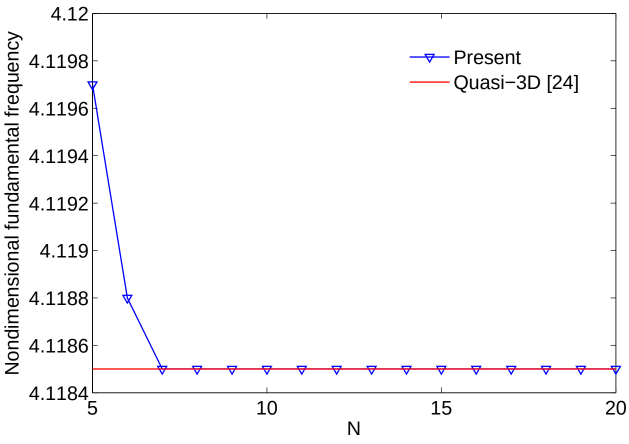

(a) S-S

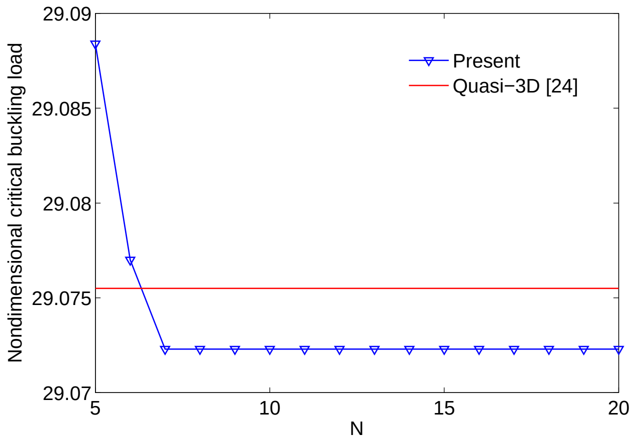

(b) S-S

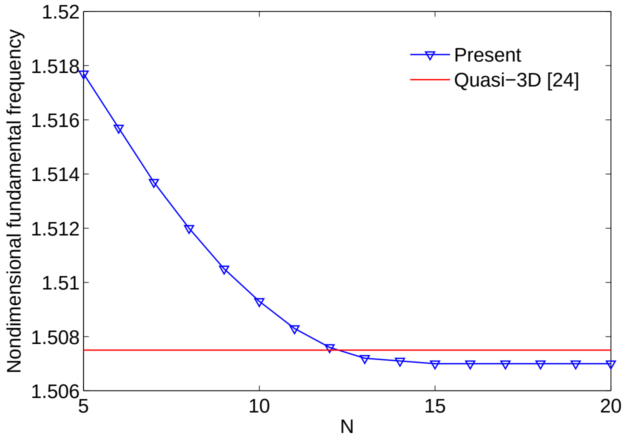

(c) C-F

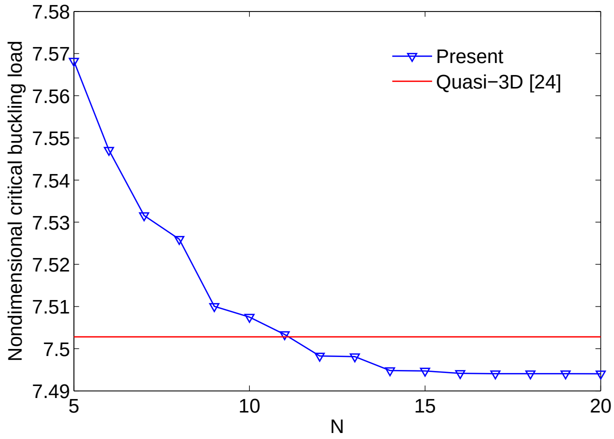

(d) C-F

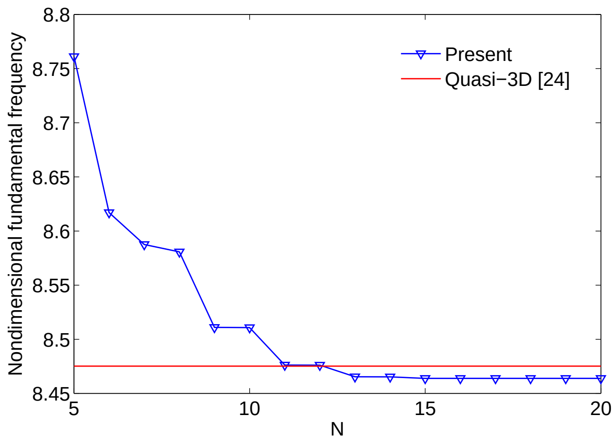

(e) C-C

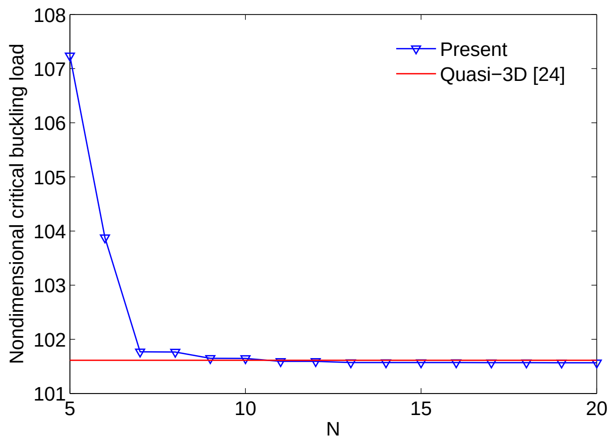

(f) C-C

Figure 2: Convergence of the nondimensional fundamental frequency ($\bar{\omega}$) and critical buckling load ($\bar{N}_{cr}$) of FG sandwich beams (type A, $p = 1, L/h = 5$).

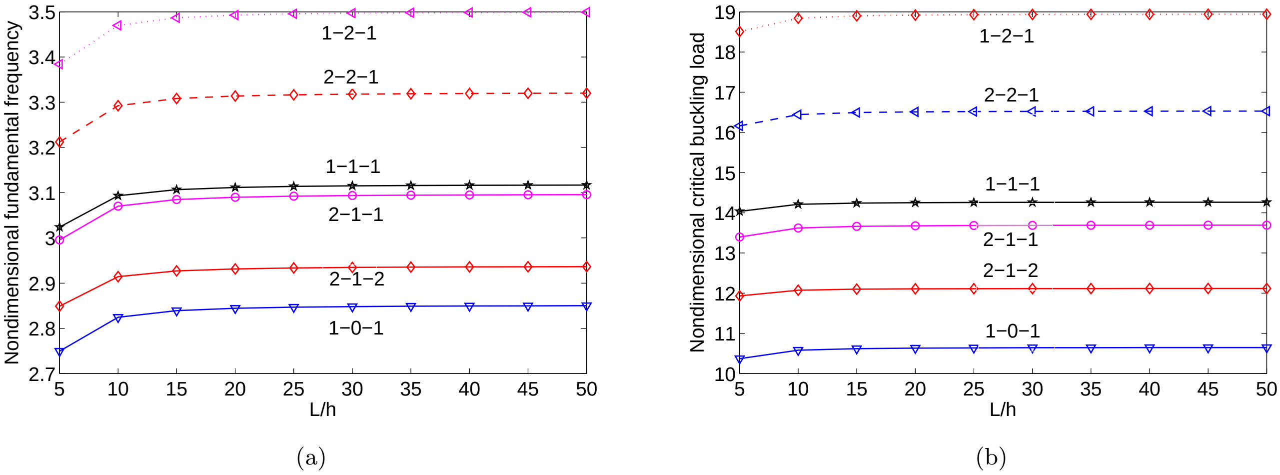

Figure 3: Effects of the span-to-depth ratio L/h on the nondimensional fundamental frequency ($\bar{\omega}$) and critical buckling load ($\bar{N}_{cr}$) of FG sandwich beams (type A, $p = 5$).

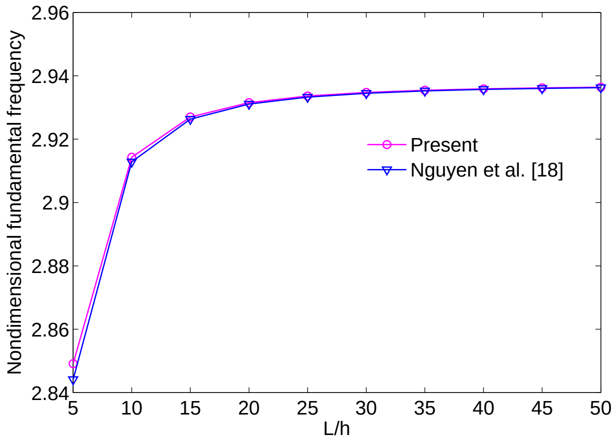

(a) S-S FG sandwich beams

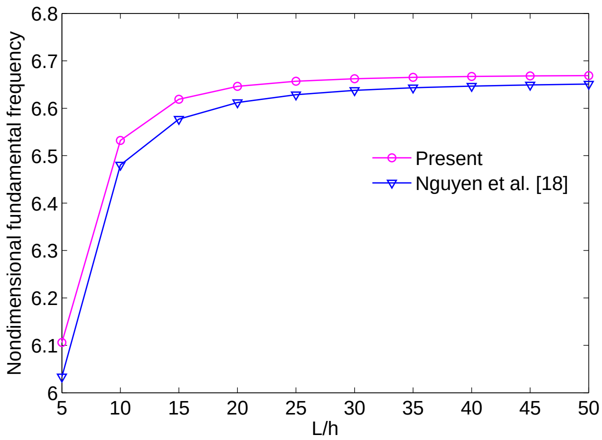

(b) C-C FG sandwich beams

Figure 4: Variation of the nondimensional fundamental frequency ($\bar{\omega}$) with respect to the span-to-depth ratio L/h of (2-1-2) FG sandwich beams (type A, $p = 5$).

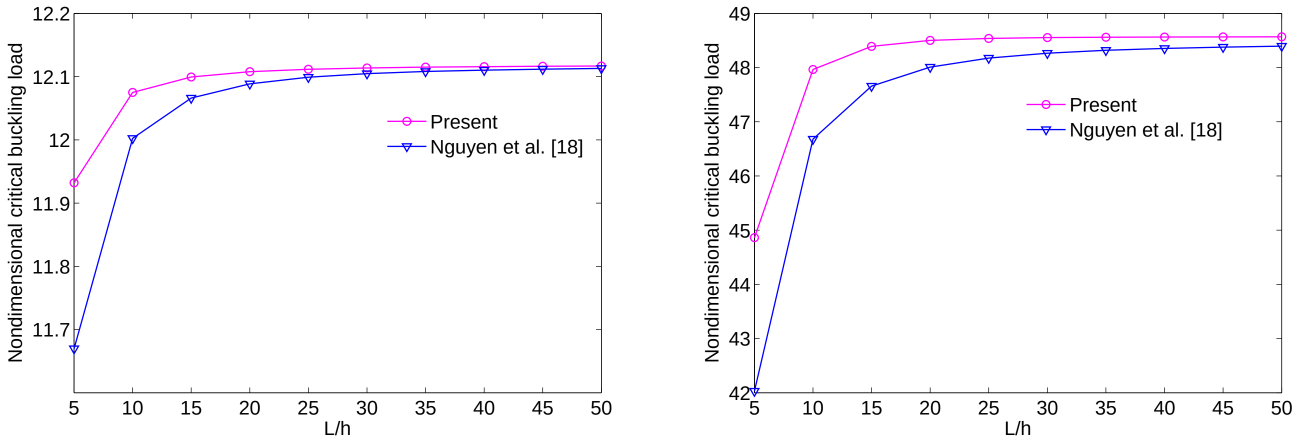

(a) S-S FG sandwich beams

(b) C-C FG sandwich beams

Figure 5: Variation of the nondimensional critical buckling load ($\bar{N}_{cr}$) with respect to the span-to-depth ratio L/h of (2-1-2) FG sandwich beams (type A, $p = 5$).

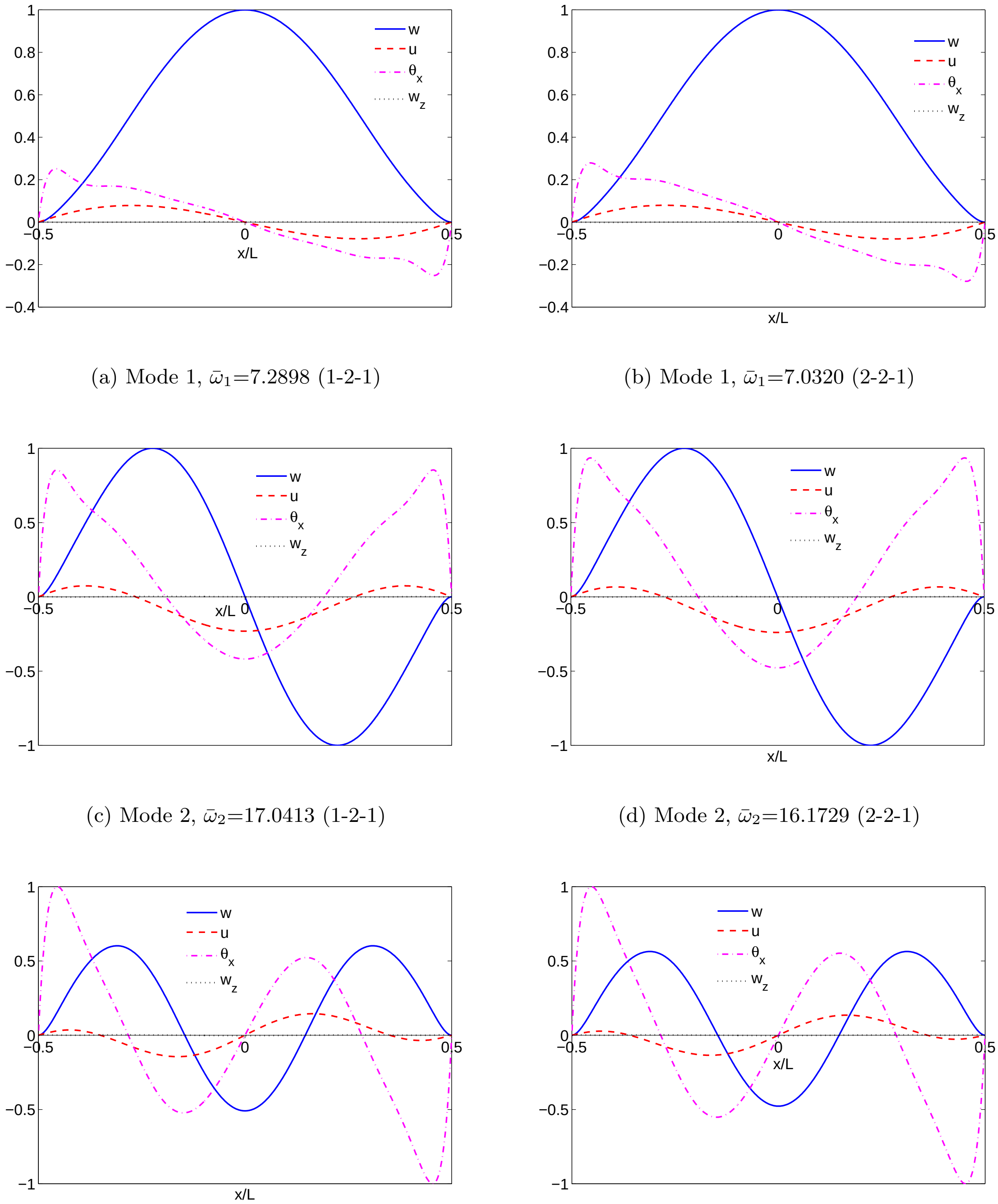

(a) Mode 1, $\bar{\omega}_1$=7.2898 (1-2-1)

(b) Mode 1, $\bar{\omega}_1$=7.0320 (2-2-1)

(c) Mode 2, $\bar{\omega}_2$=17.0413 (1-2-1)

(d) Mode 2, $\bar{\omega}_2$=16.1729 (2-2-1)

(e) Mode 3, $\bar{\omega}_3$=28.7917 (1-2-1)

(f) Mode 3, $\bar{\omega}_3$=27.0964 (2-2-1)

Figure 6: The first three mode shapes of C-C FG sandwich sandwich beams ($L/h = 5$, $p = 2$, type B).